3D-QSAR and docking studies on transforming growth factor (TGF)-β receptor 1 antagonists

Werner J. Geldenhuys [a,*], Hiroshi Nakamura [b]

[a] Department of Pharmaceutical Sciences, Northeastern Ohio Universities Colleges of Medicine and Pharmacy, 4209 State Route 44, Rootstown, OH, USA
[b] Department of Ophthalmology, Summa Health Systems, Akron, OH, USA

ABSTRACT

The transforming growth factor-β (TGF-β) is part of a family of cytokines which regulate various signaling pathways such as cell development, growth, and tissue injury. Although several studies have been published describing the synthesis of small compounds which inhibit the receptor of TGF-β, especially the subtype 1 receptor (TGBR1) kinase, no 3D-quantitiative structure–activity relationship study has been published. Here we describe the development of a comparative molecular field analysis (CoMFA) model which yielded a partial least squares statistical cross validated r^2 of >0.3. CoMFA maps agree with docking studies and pharmacophore analysis that hydrogen bonding is important for binding to ALK-5. These studies could enable the medicinal chemist to develop novel inhibitors which can be used in glaucoma filtration surgery.

Published by Elsevier Ltd.

Transforming growth factor-β (TGF-β), is a cytokine which plays an important role in multiple physiological processes. It forms part of a family of cytokines which are involved in cell growth, differentiation, and matrix expression. TGF-β can bind to one of two serine/threonine kinases, which are located in the cellular transmembrane. Two main receptors/kinases for TGF-β exist, namely TGF-β receptor type 1 and 2 (TGFBR1 and TGFBR2). The drug target we are interested in for this study, namely TGFBR1, is also commonly referred to as activin receptor-like kinase **5** (ALK-5). Unique combinations of the type I and type II receptors confer specificity of ligand signaling. TGF-β displays a high affinity for the type II receptors and do not interact with the isolated type I receptors.[1] Signal transduction of TGF-βs is initiated by binding to the type II receptor, followed by its association with TGFBR1. The activated TGFBR1 in turn phosphorylates and activates transcription factors Smad2/3.[2] TGFBR1 should therefore be reliable a target to block the TGF-β signaling pathway.

Since TGF-β seems to play an important role in several diseases ranging from cancer,[3,4] to arthrosclerosis[5] and pulmonary fibrosis,[6] it has garnered interest as a drug target. Our interest in TGF-β is borne from the investigation for the use of TGFBR1 inhibitors in glaucoma filtration surgery.[4,7] To prevent the debilitating effects of increased intra-ocular pressure of the eye in glaucoma, a drainage route can be surgically constructed for the aqueous humor to flow out to subconjunctival space. Unfortunately, one of the drawbacks of this method is post-surgical scar formation which blocks
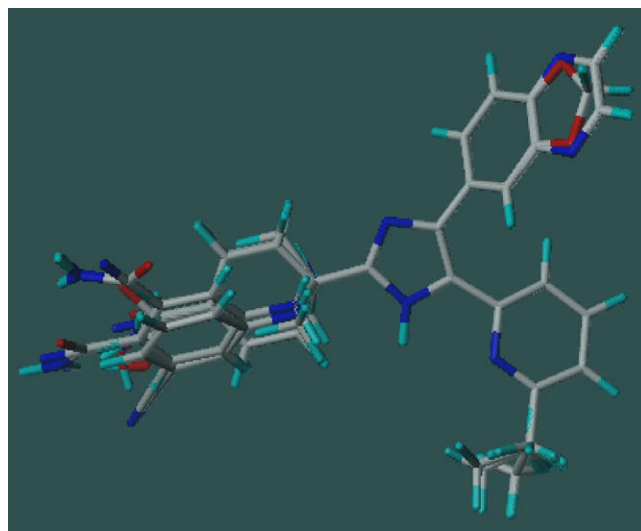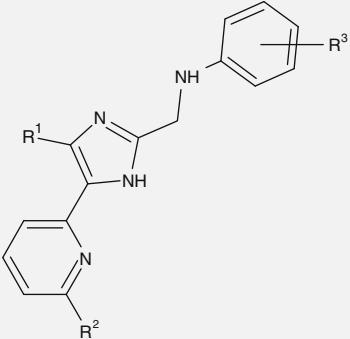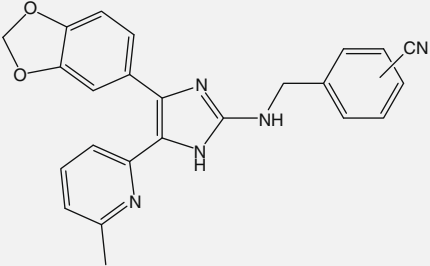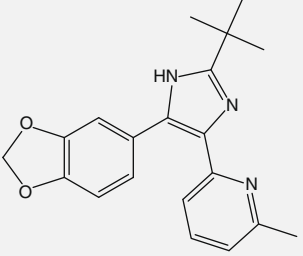

Figure 1. Alignment of the compounds used in this study.
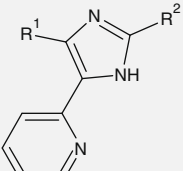
* Corresponding author. Tel.: +1 330 325 6474; fax: +1 330 325 5936.
 E-mail address: wgeldenh@neoucom.edu (W.J. Geldenhuys).

Table 1
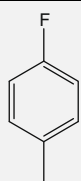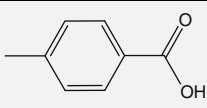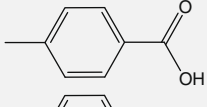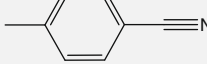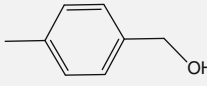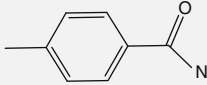Structures of the compounds used in this study, with their representative inhibitory activity of TGFBR1[10,13]

	R^1	R^2	R^3	IC_{50} (µM)
1	A	Me	m-CN	0.046
2	A	Me	p-CN	0.171
3	A	Et	m-CN	0.073
4	A	Et	p-CN	0.360
5	B	Me	m-CN	0.012
6	B	Me	p-CN	0.042
7	B	Et	m-CN	0.119
8	B	Et	p-CN	0.047
9	A	Me	m-CONH$_2$	0.021
10	A	Me	p-CONH$_2$	0.262
11	A	Et	m-CONH$_2$	0.046
12	A	Et	p-CONH$_2$	0.385
13	B	Me	m-CONH$_2$	0.010
14	B	Me	p-CONH$_2$	0.075
15	B	Et	m-CONH$_2$	0.015
16	B	Et	p-CONH$_2$	0.092
17				0.024
18				0.153

Table 1 (*continued*)

	R^1	R^2	IC_{50} (µM)
19	[4-fluoro structure]	[4-methylbenzoic acid structure]	1.5
20	A	[4-methylbenzoic acid structure]	0.17
21	A	[4-methylbenzonitrile structure]	2.95
22	A	[4-methylbenzyl alcohol structure]	0.26
23	A	[4-methylbenzamide structure]	0.094

A = benzo[1,3]dioxyl-5-yl.
B = quinoxalin-6-yl.
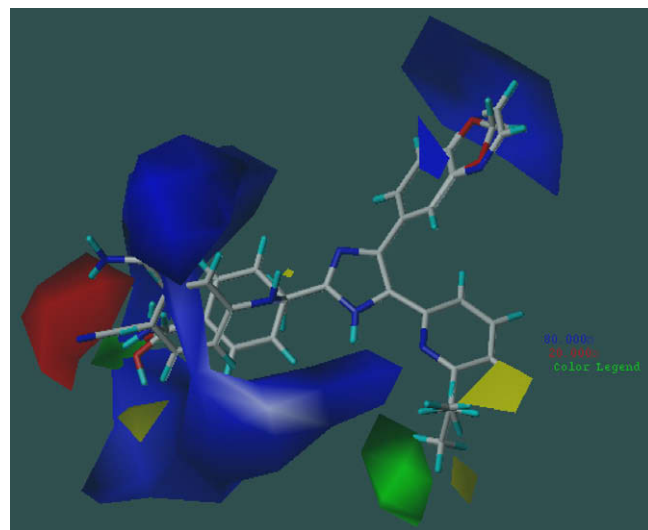
Figure 2. CoMFA maps surrounding the test set compounds. Green maps indicate areas where steric bulk is likely to increase affinity, and yellow where steric bulk will likely decrease affinity. The electrostatic maps are shown in blue (more positively charged) and red (more negatively charged).

drainage of the fluid. In a previous study, we have shown that TGFBR1 inhibitors have potential to suppress post-surgical ocular scarring in a rabbit model of glaucoma filtration surgery.[7]

Several studies have been recently been published describing the synthesis and biological activity of TGFBR1 inhibitors[8–12] (Fig. 1). Compounds such as SB-505124 and A83-01 have been shown to bind to the ATP-binding site of TGFBR1 and act as competitive inhibitors, and in cell culture have shown effective inhibition of TGF-β. Structurally, most of these compounds, which have

been published, share a similar central core consisting of a pyrazole or imidazole with a pyridine. Although structure–activity relationships have been explored by side chain modification in synthesis projects, no 3D-quantitative structure–activity relationship (3D-QSAR) study has been published to date. The current study aims to fill this void in the literature.

Molecular modeling studies were accomplished using the CoMFA module of SYBYL 8.1 and SYBYL-X (Tripos, St Louis MO), utilizing a Dell XPS720 3.66 GHz PC dual booted to run Red Hat Linux Enterprise 5 and Microsoft Windows XP. Molecules taken from the literature[10,13] were drawn and energy-minimized in SYBYL using the MMFF94s force field with Gasteiger–Hückel charges added. The compounds used in this study were aligned with SB-505124 as a template. To ensure that the influence of side chains can be accurately measured with the CoMFA method, the core of SB-505124 was made an aggregate. This allowed for the side chains to be optimized after each compound was sketched.

Default values provided in the Tripos CoMFA module were used with a 2.0 Å grid spacing using a sp^3 carbon atom with a +1 point charge as a probe to explore the steric and electrostatic interactions at the lattice points in the grid. The default cut-off value was set at 30 kcal/mol. Statistical analysis was performed using the partial least squares method implemented in the SYBYL program. Non-cross validated (r^2) values were determined for the models using linear regression analysis (with variances reported as the standard error of estimation, S.E.E.) which are considered significant when r^2 is greater than 0.7. The q^2 values obtained were considered significant at 0.3. The 3D graphical representation of the steric and electrostatic fields generated through CoMFA are shown with the relative contributions represented as a 3D coefficient map with favored 80% steric (green) and electrostatic (blue) effects and 20% disfavored steric (yellow) and electrostatic effects (red). Green colored areas of the map indicate where sterically bulky groups may enhance interaction affinity. Blue colored areas (80%) indicate regions where a more positively charged group will likely lead to increased binding affinity, while red areas indicate where a more negatively charged group will likely lead to increased binding (20%). Biological data were entered as log K_i values in the spreadsheets accessed by the CoMFA routine in SYBYL. Compound **16** was removed as an outlier from the final model generation.

For the docking study, we used GOLD v. 4.1 (www.ccdc.cam.ac.uk) with the 1VJY.pdb[8] crystal complex. SB-505124 was drawn with MarvinSketch v. 5.2 (www.chemaxon.com) and imported into MOE v. 2009.10 (Chemical Computing Croup, http://www.chemcomp.com) where the compound was energy-minimized with the MMFF94s force filed with a termination criterion of 0.001 kcal/mol, and saved in the correct format for use in GOLD. In GOLD, the protein and the ligand of 1VJY were separated, while hydrogens were added to the protein. Since water seems to play a role in binding to the ATP pocket of kinase binding, we did not delete the water. The top poses were inspected with PyMol v. 0.99 (www.pymol.org). To identify the ligand–protein interactions, the top pose and protein were loaded into MOE and the LigX function was run to investigate the interactions.

Table 2
Results from the CoMFA analysis on the TGFBR1 inhibitors

q^2 Cross validated	0.438
SEP	0.508
Number of components	4
Non-cross validated r^2	0.921
SEE	0.191
F (n_1 = 4; n_2 = 13)	37.651
Steric contribution	0.387
Electrostatic contribution	0.613

Table 3
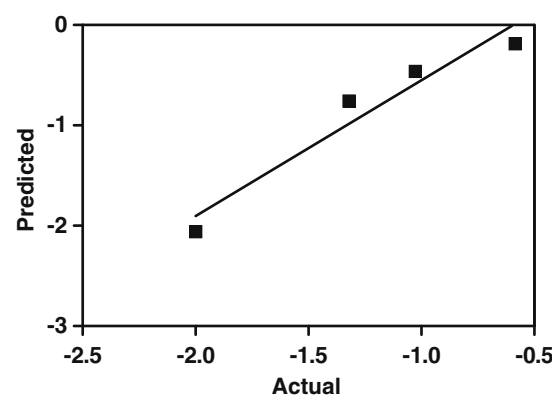Predicted values for the test set compounds from the CoMFA analysis

Compound	Experimental log K_i (μM)	Predicted log K_i (μM)
22	−0.585	−0.186
23	−1.027	−0.462
8	−1.32	−0.756
13	−2	−2.06
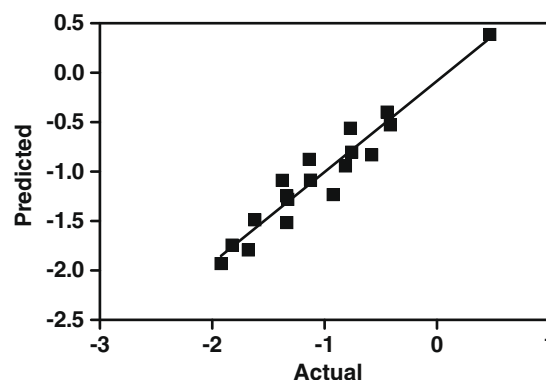
Figure 3. Correlation between the actual and predicted values for the training set using to build the CoMFA model. The statistics of the model is given in Table 2.

Table 4
Biological activity of kinase inhibitors of TGFBR1, as well as their predicted activity from the CoMFA analysis

| Compound	LOGIC50	PRED	Residual
20	−0.77	−0.558	0.212
21	0.4698	0.389	−0.0808
1	−1.337	−1.515	−0.178
2	−0.759	−0.802	−0.043
3	−1.137	−0.874	0.263
4	−0.4434	−0.396	0.0474
5	−1.921	−1.929	−0.008
6	−1.377	−1.086	0.291
7	−0.924	−1.231	−0.307
9	−1.678	−1.791	−0.113
10	−0.582	−0.829	−0.247
11	−1.337	−1.243	0.094
12	−0.415	−0.527	−0.112
14	−1.125	−1.084	0.041
15	−1.824	−1.741	0.083
17	−1.62	−1.485	0.135
18	−0.815	−0.941	−0.126
SB-505124	−1.328	−1.279	0.049

Figure 4. Correlation between the actual and predicted values from the external test set (Table 3) of compounds. The resulted correlation coefficient (r^2) = 0.936.

TGFBR1 is an attractive drug target for multiple diseases such as in the use of glaucoma infiltration surgery. The last few years have seen a steady increase in the medicinal chemistry literature describing the synthesis of new compounds which may act as inhibitors. The current study was done to fill a large gap in the TGFBR1 literature since no 3D-QSAR study has been published.

When the literature was evaluated to identify inhibitors of TGFBR1, it was found that most of the publications had few compounds which had been tested against TGFBR1. Although larger sets do occur, the scaffold structure is different between the groups discussed. Since CoMFA works best with congeneric series, we focused on the series presented here in Table 1, to investigate which areas can be used for side chain/R-group modification most likely to increase activity. In this study, the CoMFA models, which were generated, are presented in Figure 2 with the results of the statistics given in Table 2. The developed CoMFA model gave a signifi-

cant cross validated regression value of 0.438 with a standard error of prediction of 0.508. This partial least squares analysis suggested that the number of components to use in the non-cross validated regression model was four components. The resulting non-cross validated linear regression model gave a value of 0.92 and a standard error of estimate of 0.191 (Fig. 3). The predicted activity values for the training set compounds are shown in Table 4. The steric and electrostatic contributions were found to be 39% and 61%, respectively. To validate this CoMFA model, we used a small test set which was not used in the training of the model (Fig. 4 and Table 3). As can be seen from the correlation between the CoMFA predicted and experimental values, there was a strong correlation (r^2 >0.7), suggesting this model has the capability to predict the affinity of new compounds with similar structural features. The favoring of electrostatics seen in this CoMFA model corroborates the finding that hydrogen bonding plays a large role
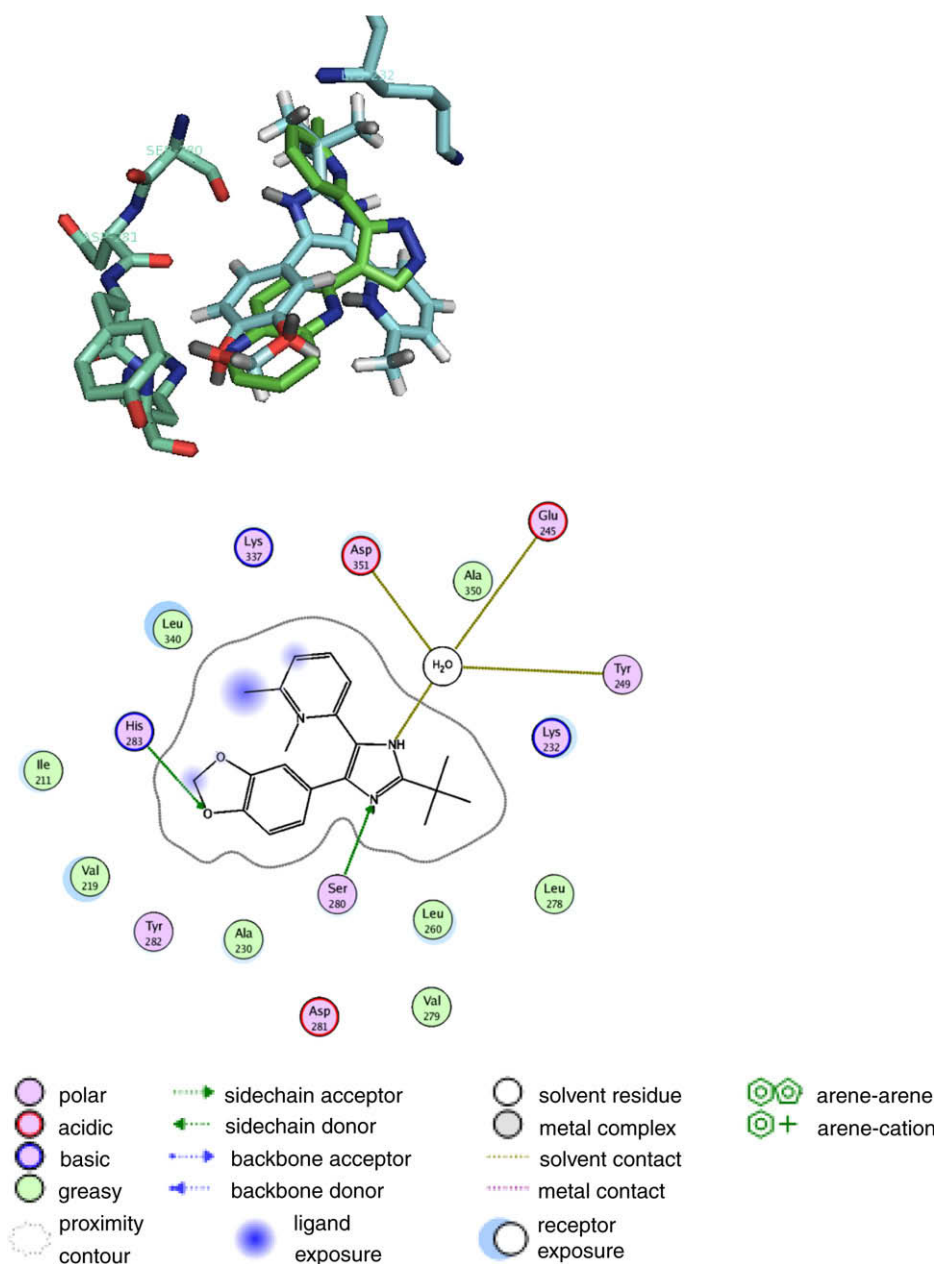
Figure 5. Docking results of SB–505124, a potent TGFBR1 inhibitor (TGF-β receptor 1), in the crystal structure of TGFBR1 (access code: 1VJY.pdb). The original ligand of 1VJY, a 1,5-naphthyridine compound (in green), is also shown.[8] The amino acid residues which are thought to interact with SB–505124 are shown also as a 2D representation using LigX in MOE.
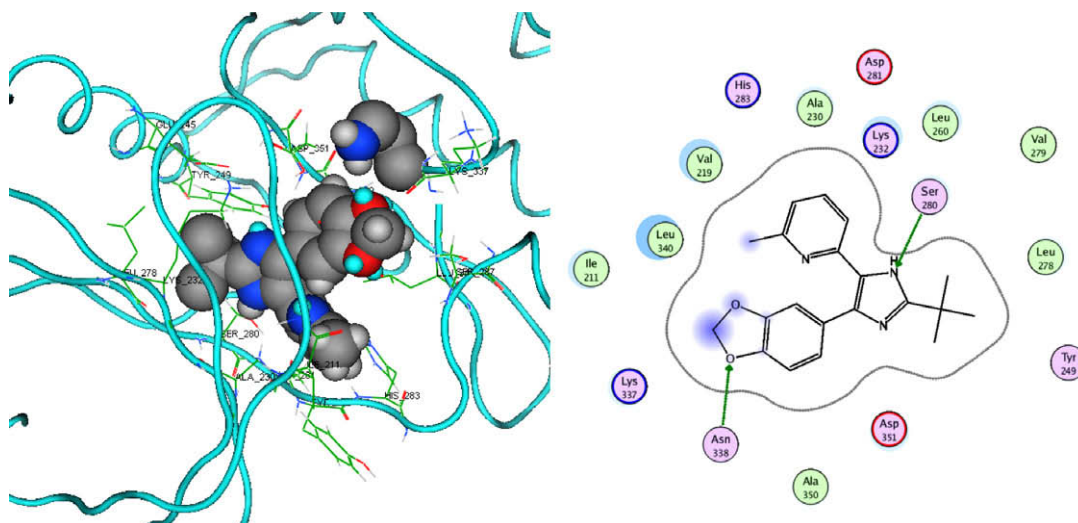
Figure 6. The amino acid ASN338 may also be able to interact with SB-505124. As depicted with space filling, one of the rotamers is able to orient for hydrogen bonding between the ligand and the protein.
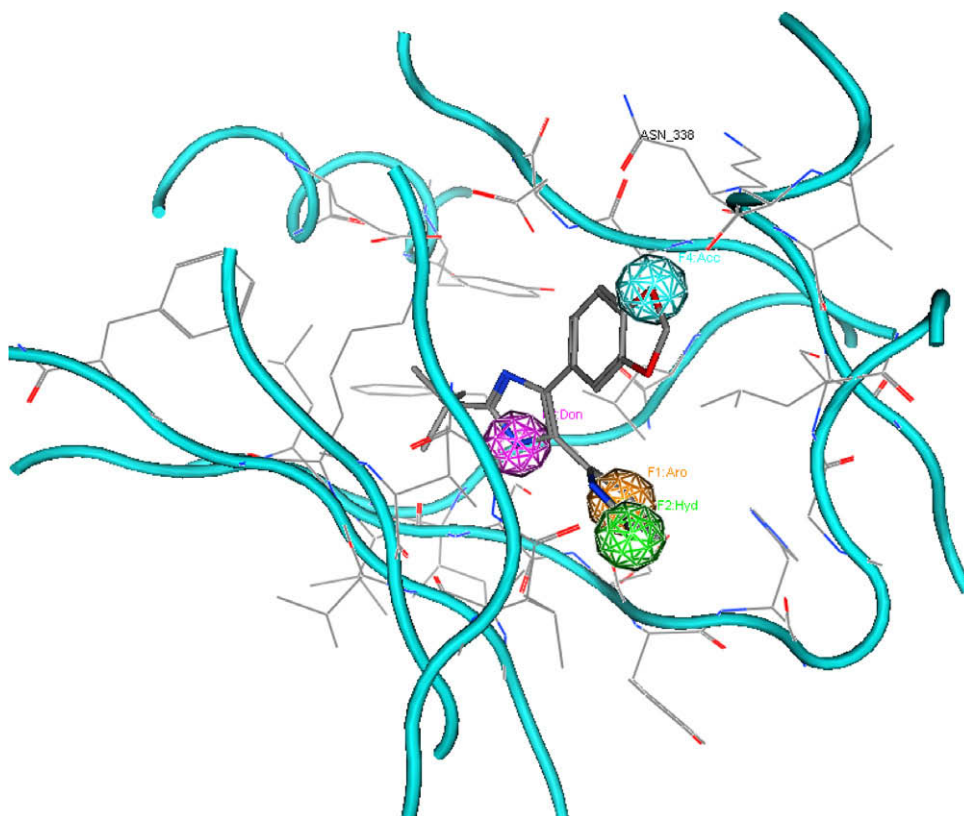
Figure 7. Pharmacophore points shown on SB-505124, indicating hydrogen bond acceptor and donating groups which may play a role in the activity of these compounds.

in kinase binding, as opposed to pure steric bulk of a compound fitting in the pocket. The CoMFA maps (Fig. 2) are dominated by electrostatic areas, which was shown by the non-linear regression statistics. Green colored areas of the map indicate where sterically bulky groups may enhance interaction affinity. Blue colored areas (80%) indicate regions where a more positively charged group will likely lead to increased binding affinity while a red area indicates where a more negatively charged group will likely lead to increased binding (20%). The large blue areas mostly surround nitrogen containing atoms in the compounds, either by virtue of their

ability to be protonated at physiological pH, or that they may contribute to hydrogen bonding. In contrast, only a single area which has a red map indicates where negatively charged groups will be likely to increase affinity. This is probably due to the number of oxygen containing R-groups in this set, suggesting that they interact via a possible hydrogen/charge bond in the general area. In contrast to the large electrostatic maps seen in the CoMFA maps, are the smaller more concentrated steric maps. As can be seen in Figure 2, an area for increased steric bulk is located *ortho* to the aromatic nitrogen. This would explain the affinity for example

compound, which has an aliphatic substituent in that area. In contrast, the *meta* position from the aromatic nitrogen would disfavor any increases in affinity, and is suggested to have a negative impact on a compounds ability to bind to the TGFBR1 binding pocket.

The lead compound for this study, SB-505124 was docked to the ATP-binding pocket of TGFBR1 using GOLD (Fig. 5). We chose to use this docking program because it has a scoring function which is specifically parameterized for kinases. Validation of this docking procedure returned the co-crystallized compound with a RMSD which was less than 1 Å. The top binding pose returned from the docking studies shows a similar orientation in the binding pocket to the co-crystallized 1,5-napthyridine compound found in 1VJY.pdb. A possible hydrogen bonding interaction appears to be possible between amino acids His-283 as well as Ser-280. Additionally, there is a water molecule which seems to form a hydrogen bridge- bonding interaction between SB-505124 and Asp-351, Glu-245 and Tyr-249.

These results from the docking study corroborate the findings of the CoMFA model, in that hydrogen bonds are important for this kinase interaction, and virtual screening databases will need to account for hydrogen bond donating and accepting groups. Larger more bulky groups may not be able to interact with TGFBR1 simply due to the fact that it may not fit in the ATP-binding pocket, and therefore are excluded from binding.

Another observation from the docking studies was that the amino acid Asn-338 was found to be in proximity to the oxygens in SB-505124. Although the crystal structure of TGFBR1 which we used here for docking, (1VJY.pdb), showed Asn-338 to have its nitrogen pointing away from the oxygens in SB-505124, rotamer sampling of the amino acid with MOE indicated that this amino acid has the possibility to rotate and form a hydrogen bond with the inhibitor. Re-minimization of the TGFBR1-SB-505124 complex indicates that this bond is possible (Fig. 6). Movement of one or more side chains in the binding pocket of a kinase, such as suggested from our studies, have been seen with other kinases, such as CDK2 and has been described previously in the work from Sherman et al.[14] Taking this into account, a pharmacophore model for binding to TGFBR1 was constructed which was found to corroborate the findings in the CoMFA studies. As seen in Figure 7, there is a hydrogen bond donating pharmacophore sphere positioned at the imidazole ring of SB-505124, and a hydrogen bond acceptor on the oxygens. Taken together, it seems that the pyrazole/imidazole hydrogen bond-pyridine aromatic/aliphatic combination may be the driving force of initial orientation within the ATP-binding site,

and increase in affinity can be afforded by the addition of at least one or more hydrogen bond donor/acceptor groups.

In conclusion, here for the first time we present a 3D-QSAR model of the TGFBR1 kinase binding site using a small set of ligands. The major conclusion from these models, in conjunction with the docking solutions, was that hydrogen bonding groups play a large role in the affinity for the kinase. By adding these groups to new compounds, high affinity compounds will likely result, as opposed to the introduction of large sterically dominating groups. The results in this study should aid in the understanding of structure–activity relationships with this important kinase and in future drug discovery projects to identify novel compounds, which we are currently working towards.

Acknowledgments

References and notes

1. Massague, J. *Annu. Rev. Biochem.* **1998**, *67*, 753.
2. Seuntjens, E.; Umans, L.; Zwijsen, A.; Sampaolesi, M.; Verfaillie, C. M.; Huylebroeck, D. *Cytokine Growth Factor Rev.* **2009**.
3. Kaminska, B.; Wesolowska, A.; Danilkiewicz, M. *Acta Biochim. Pol.* **2005**, *52*, 329.
4. Saika, S. *Lab. Invest.* **2006**, *86*, 106.
5. Feinberg, M. W.; Jain, M. K. *Panminerva Med.* **2005**, *47*, 169.
6. Ask, K.; Martin, G. E.; Kolb, M.; Gauldie, J. *Proc. Am. Thorac. Soc.* **2006**, *3*, 389.
7. Sapitro, J.; Donmire, J.; Sutariya, J.; Geldenhuys, W. J.; Yue, B. Y. J. T.; Nakamura, H. *Mol. Vis.* **2009**.
8. Gellibert, F.; Woolven, J.; Fouchet, M. H.; Mathews, N.; Goodland, H.; Lovegrove, V.; Laroze, A.; Nguyen, V. L.; Sautet, S.; Wang, R.; Janson, C.; Smith, W.; Krysa, G.; Boullay, V.; De Gouville, A. C.; Huet, S.; Hartley, D. *J. Med. Chem.* **2004**, *47*, 4494.
9. Sawyer, J. S.; Beight, D. W.; Britt, K. S.; Anderson, B. D.; Campbell, R. M.; Goodson, T., Jr.; Herron, D. K.; Li, H. Y.; McMillen, W. T.; Mort, N.; Parsons, S.; Smith, E. C.; Wagner, J. R.; Yan, L.; Zhang, F.; Yingling, J. M. *Bioorg. Med. Chem. Lett.* **2004**, *14*, 3581.
10. Callahan, J. F.; Burgess, J. L.; Fornwald, J. A.; Gaster, L. M.; Harling, J. D.; Harrington, F. P.; Heer, J.; Kwon, C.; Lehr, R.; Mathur, A.; Olson, B. A.; Weinstock, J.; Laping, N. J. *J. Med. Chem.* **2002**, *45*, 999.
11. Gellibert, F.; de Gouville, A. C.; Woolven, J.; Mathews, N.; Nguyen, V. L.; Bertho-Ruault, C.; Patikis, A.; Grygielko, E. T.; Laping, N. J.; Huet, S. *J. Med. Chem.* **2006**, *49*, 2210.
12. Sawyer, J. S.; Anderson, B. D.; Beight, D. W.; Campbell, R. M.; Jones, M. L.; Herron, D. K.; Lampe, J. W.; McCowan, J. R.; McMillen, W. T.; Mort, N.; Parsons, S.; Smith, E. C.; Vieth, M.; Weir, L. C.; Yan, L.; Zhang, F.; Yingling, J. M. *J. Med. Chem.* **2003**, *46*, 3953.
13. Kim, D. K.; Jang, Y.; Lee, H. S.; Park, H. J.; Yoo, J. *J. Med. Chem.* **2007**, *50*, 3143.
14. Sherman, W.; Day, T.; Jacobson, M. P.; Friesner, R. A.; Farid, R. *J. Med. Chem.* **2006**, *49*, 534.